# Selective Preparation of Furfural *via* the Pyrolysis of Cellulose Catalyzed with Nitrided HZSM-5

Xinluan Wang, Shanjian Liu, Deli Zhang, Dongmei Bi, Lihong Wang, Jiaqi Zhang, and Weiming Yi *

Furfural is a high-value compound that can be prepared by catalytic pyrolysis of biomass. In order to improve the selectivity of furfural in the process of cellulose catalytic pyrolysis, the ammonia-modified HZSM-5 (N-HZSM-5) was used as the catalyst for experimental research on a horizontal fixed bed. The effects of different nitriding temperatures and times on N-HZSM-5, and the effects of different catalyst to cellulose (CA to CL) ratios on furfural selectivity were evaluated. The results showed that N-HZSM-5 can effectively improve the selectivity for furfural. At the optimal conditions (nitriding temperature: 800 °C, nitriding time: 6 h, CA to CL ratio: 4), the selectivity of furfural was up to 24%, which was much higher than those of noncatalytic pyrolysis (1.2%) and HZSM-5 catalytic pyrolysis (3.6%). In order to better evaluate the performance of the catalyst, a series of characterizations were carried out on the N-HZSM-5. The results showed that compared with HZSM-5, N-HZSM-5 had an increased pore size, it was less acidic, and it had more uniform surface acidity. It was conducive to the selective formation of furfural. Therefore, the ammonia-modification can effectively control the structure and acidity of HZSM-5, and N-HZSM-5 exhibits a non-negligible potential in catalyzing the pyrolysis of cellulose for furfural.

*Keywords: Cellulose; Catalytic pyrolysis; Furfural; Nitrided HZSM-5; Selective regulation*

*Contact information: School of Agricultural Engineering and Food Science, Shandong Research Center of Engineering & Technology for Clean Energy, Shandong University of Technology, Zibo 255000 China; * Corresponding author: yiweiming@sdut.edu.cn*

## INTRODUCTION

Biomass is an environment-friendly, low cost, and renewable resource; its reasonable development and utilization is the only way to realize a low-carbon economy (Kabir and Hameed 2017; Zhang *et al*. 2018; Razzaq *et al*. 2019). Cellulose is the primary component of biomass. It has a wide range of sources and a simple structure. In addition, it can achieve high-value applications through pyrolysis technology, which is of great research importance (Liang *et al*. 2011). The primary products of cellulose pyrolysis are levoglucan (LG), levoglucosidone (LGO), hydroxylactone (LAC), and furfural (FF) (Lu *et al*. 2011b; Gao *et al*. 2019; Li *et al*. 2021). Among them, furfural can be used to produce medicines, resins, and fuel additives, and it is considered as one of the most promising chemicals for the sustainable production of fuels and chemicals in the 21$^{st}$ century. It can also be a good extractant, and at the same time, a precursor of various furan chemicals, which will be in considerable demand in the future (Lange *et al*. 2012; Cai *et al.* 2013; Lu *et al*. 2013; Chen *et al*. 2017).

In recent years, extensive studies have been conducted on the production of furfural *via* the catalytic pyrolysis of biomass, including the application of various catalysts, *e.g.*,

acid salts, organic/inorganic acids, and solid acids. Among them, homogeneous acid catalysts, *e.g.*, solutions of $ZnCl_2$, $H_2SO_4$, and ammonium dihydrogen phosphate, can effectively improve the selectivity of furfural. Lu *et al.* (2011a) used $ZnCl_2$ to impregnate biomass and pyrolyzed it to produce furfural at a low temperature. The maximum peak area percentage of furfural was greater than 70%. Fan *et al.* (2018) quickly pyrolyzed corncob impregnated with $H_2SO_4$, and under optimal process conditions, the furfural yield reached 19.18 wt%. Li *et al.* (2020) reported that ammonium dihydrogen phosphate showed good selectivity for the preparation of furfural and levoglucosidone from biomass pyrolysis, and the total relative peak area reached 52.23%. Although a homogeneous acid catalyst catalyzes the pyrolysis of biomass to obtain higher yields of furfural, the catalysis process suffers from some problems, mainly corrosiveness, difficulty in recycling the catalyst, and low economic feasibility. In contrast, heterogeneous solid acid catalysts are relatively friendly to the environment, and it is easier to recycle the catalysts. Accordingly, they have a wide range of application prospects. Chen *et al.* (2018) used a series of SAPO catalysts for the rapid pyrolysis of cellulose and found that ZrCu-SAPO-18 has the best selectivity for furfural formation, up to 27.59%. Zhang *et al.* (2014) found that the catalyst $CuSO_4$/HZSM-5 can promote the degradation of polysaccharides into furfural with a maximum yield of 28%. Among them, HZSM-5, with its excellent shape-selective catalytic ability and strong acidity, is the primary research hotspot of biomass catalytic pyrolysis at this stage (Fanchiang *et al*. 2012; Veses *et al.* 2015; Shahsavari and Sadrameli 2020). However, during cellulose catalytic pyrolysis, the strongly acidic active sites of HZSM-5 can easily cause excessive reactions, which will further convert furfural and other furan compounds into aromatics and olefins, which is not conducive to the selective preparation of furfural. At the same time, its smaller pore size distribution and carbon deposition problems will also reduce the catalyst life (Zhang *et al*. 2020).

Therefore, for cellulose catalytic pyrolysis to prepare furfural, it is necessary to modify the pore structure and acidity of the HZSM-5 catalyst. Since 1968, nitriding has been used to change the structure and acidity of zeolite molecular sieves (Lyu *et al*. 2017). Presently, the most commonly used method for preparing nitrogen-containing molecular sieves is to directly place the molecular sieves in a high-temperature $N_2$ or $NH_3$ atmosphere. Compared with $N_2$, the more active $NH_3$ is used as the nitrogen source, because the $NH_3$ atmosphere may be more conducive to maintaining the stability of the molecular sieve framework at high temperatures (Narasimharao *et al*. 2006). Therefore, ammonia modification is worth considering. Moreover, ammonia modification is relatively mild compared with traditional immersion modification; the distribution of acidic sites on the surface may be more uniform. Therefore, ammonia modification has considerable research potential in the highly selective preparation of furfural from cellulose catalytic pyrolysis. However, to the best of the knowledge of the authors, the preparation characteristics of ammonia-modified HZSM-5 (N-HZSM-5) as well as the subsequent furfural formation during the catalytic pyrolysis of biomass have not been evaluated. Therefore, it has certain scientific importance to evaluate the selective preparation of furfural from biomass through the catalytic pyrolysis of nitrogen-rich HZSM-5 modified with ammonia.

Based on the above analysis, the effect of N-HZSM-5 catalyzed pyrolysis of cellulose on the selectivity of furfural was evaluated for the first time. First, N-HZSM-5 catalysts prepared under different nitriding temperatures and different nitriding times were evaluated and compared. Based on the prepared N-HZSM-5 catalyst, the catalyst was screened for furfural selectivity as the primary evaluation index, and a series of cellulose catalytic pyrolysis experiments were carried out in a horizontal tube furnace. To optimize

the catalytic pyrolysis conditions for the preparation of furfural, the effect of the catalyst to cellulose (CA to CL) ratio on the catalytic reaction was evaluated. Finally, based on the experimental data and the catalyst characterization results, the possible reaction pathways of N-HZSM-5 catalyzed *via* the pyrolysis of cellulose to furfural were explored. This study will be beneficial for the highly selective preparation of furfural *via* cellulose catalytic pyrolysis.

## EXPERIMENTAL

### Materials

The α-cellulose (CAS #: 9004-34-6) purchased from Aladdin Industrial Corporation (Ontario, CA) is a white powder with an average particle size of 50 μm. Before the experiment, the cellulose was dried in an oven at a temperature of 105 °C overnight and then moved to a dryer for use. The HZSM-5 molecular sieve (Si/Al = 25) was purchased from Nankai University. Before the experiment, the HZSM-5 sieve was roasted in a muffle furnace at a temperature of 550 °C for 5 h.

### Catalyst Preparation

A certain amount of HZSM-5 was weighed, spread flat on a quartz boat, and placed in the middle area of a tubular resistance furnace, which was slowly heated up and $N_2$ was introduced at a flow rate of 100 mL/min. When the required temperature, *i.e.*, 600 °C, 700 °C, 800 °C, or 900 °C, was reached, the $N_2$ flow was stopped. The $NH_3$ was introduced at a flow rate of 100 mL/min and the $NH_3$ flow was stopped after a certain reaction time, *i.e.*, 2 h, 4 h, 6 h, or 8 h. The product was naturally cooled to room temperature under a $N_2$ atmosphere. Thus, the N-HZSM-5 was prepared and then stored in a dryer for later use.

### Catalyst Characterization

The N-HZSM-5 and HZSM-5 catalysts were characterized *via* a full analysis of their micropores (BET), elemental analysis, scanning electron microscopy (SEM), X-ray diffraction (XRD) analysis, a $NH_3$ temperature-programmed desorption ($NH_3$-TPD) study, and pyridine adsorption infrared (Py-IR) spectroscopy.

*X-ray diffraction (XRD) analysis*

The crystal structure of the catalyst was evaluated using a polycrystalline X-ray diffractometer (Bruker AXS D8 Advance, Karlsruhe, Germany). Cu-Kα radiation was generated at 40 kV and 50 mA, with $2\theta$ varying between 3° and 50° at 0.02 °/min.

*$NH_3$ temperature-programmed desorption ($NH_3$-TPD) analysis*

An AutoChem II 2920 (Micromeritics, Norcross, GA) apparatus was used for the $NH_3$-TPD analysis to measure the acid properties of the catalyst. A sample of 50 mg was preheated at a temperature of 550 °C with a He flow (30 mL/min) for 30 min to remove the adsorbed moisture from the sample. The sample was then cooled to a temperature of 100 °C and allowed to adsorb $NH_3$ at a temperature of 100 °C for approximately 60 min until saturation. Finally, after obtaining a stable baseline, under the purge of He gas, the sample was heated to a temperature of 700 °C at a rate of 10 °C/min for desorption. The desorbed $NH_3$ was monitored using a thermal conductive detector (TCD) during the TPD process.

*Pyridine adsorption infrared (Py-IR) analysis*

The Py-IR analysis was performed with a VECTOR 22 FT-IR spectrometer (Bruker, Billerica, MA) to further quantitatively analyze the type of acid sites. The temperature of the sample used was raised to 400 °C, and the sample was vacuumed (10 to 2 Pa) for 1 h. After that, the sample was cooled down to room temperature and pyridine was adsorbed for 30 min. The spectra were recorded at a temperature of 150 °C, which was also the desorption temperature.

*BET analysis*

An ASAP 2020 analyzer (Micromeritics, Norcross, GA) was used to characterize the specific surface area, pore volume, and pore size characteristics of the catalyst. The catalyst was first degassed at a temperature of 300 °C for 3 h, and then it was subjected to a nitrogen adsorption test at a temperature of -196 °C. The specific surface area was calculated by the Barrett-Emmett Teller (BET) method, and the pore volume and average pore diameter were calculated by the Barrett-Joyner-Halenda (BJH) method.

*SEM analysis*

A FEI Sirion 200 scanning electron microscope (Thermo Fisher Scientific, Waltham, MA) was used to obtain the microstructure of the catalyst under a scanning voltage of 3.0 kV.

*Element analysis*

The element analysis was performed on the Vario EL cube type element analyzer (Elementar, Langenselbold, Germany). The test temperature was 1000 °C, while oxygen and a high temperature oxidizer were used as additives; each sample was tested twice.

## Pyrolysis Experiments

A pyrolysis device is primarily composed of a carrier gas device, horizontal tube horizontal reactor, temperature controller, and cooling system. The pyrolysis reactor was a quartz tube (700 mm × Φ 60 mm × 3 mm). The cooling system consisted of two cold traps and a cooling box. The cooling medium was ethylene glycol and water (V to V ratio of 1 to 2) at a temperature of -10 °C. The pyrolysis temperature was at 500 °C, and the amount of cellulose was controlled at 1 g. By changing the amount of catalyst, the CA to CL ratio was set to 0, 1, 2, 3, 4, and 5. Before each pyrolysis experiment, the tubular reactor was purged with high-purity nitrogen (99.999%) at a flow rate of 800 mL/min for a period of time. Once the reactor temperature reached the set value (500 °C), the quartz boat was immediately pushed into the pyrolysis zone. The process lasted for 10 min and then was maintained for an additional 5 min to ensure that the reaction was complete. Finally, the reactor was cooled to room temperature in a nitrogen atmosphere, and the yields of all the products were calculated *via* mass balance calculation. Each pyrolysis experiment was performed three times. When the deviation exceeded 5%, another pyrolysis experiment was performed.

## Bio-oil Analysis

The composition of the bio-oil was analyzed *via* gas chromatography-mass spectrometry (8890-5973, Agilent, Santa Clara, CA). A DB-1701 capillary column (60 m × 0.25 mm × 0.25 μm) was used to separate the bio-oil components. The temperature of the injector and the AUX were set to 280 and 230 °C, respectively. The GC oven was

heated from 40 to 240 °C at a rate of 5 °C/min and then maintained at that temperature for 5 min. The carrier gas was high purity helium (99.999%), and the constant flow rate was 1 mL/min. The mass spectrometry analysis was carried out in EI mode. The ionization energy was 70 eV, and the scanning range was (*m*/*z*) 12 to 750 amu. Based on the NIST 17 library, the detailed chemical information corresponding to the chromatographic peak was determined. In each experiment, the chromatographic peak area of each product was recorded, and then the relative content (peak area %) was calculated by dividing the peak area (target product) by the total peak area (all tested products). The peak area % was used to represent the selectivity of the product (Fabbri *et al.* 2007).

## RESULTS AND DISCUSSION

### Effect of Nitriding on the Texture Properties of HZSM-5

First, the effect of the nitriding temperature on the texture of the HZSM-5 sieve was evaluated. Four temperatures, *i.e.*, 600 °C, 700 °C, 800 °C, and 900 °C, were selected for nitriding HZSM-5 with a nitriding time of 4 h, which were expressed as N-HZSM-5-600, N-HZSM-5-700, N-HZSM-5-800, and N-HZSM-5-900, respectively. Table 1 shows that as the nitriding temperature increased, the nitrogen content first increased and then decreased. When the nitriding temperature was 800 °C, the nitrogen content reached up to 0.66 wt%. When the nitriding temperature was 900 °C, the nitrogen content decreased compared to lower nitriding temperatures. This was because the molecular sieve reacts with ammonia at high temperatures to produce water. In addition, the amine groups that have entered the molecular sieve may react with water to release nitrogen in the form of ammonia, so the nitrogen content is reduced (Blasco *et al*. 1999). Within the nitriding temperature range selected in the experiment, the specific surface area and pore volume of molecular sieve after nitriding showed a decreasing trend, but the change was minimal. Only when the nitriding temperature was higher (900 °C) was the specific surface area of the obtained nitrogen-containing molecular sieve considerably reduced (325 $m^2/g$). The average pore size showed the opposite trend, *i.e.*, gradually increasing with the increase in nitriding temperature, reaching a maximum value (2.75 nm) at a nitriding temperature of 900 °C. Table 1 also shows the effect of the nitriding time on the structure of the HZSM-5 sieve. Four time periods, *i.e.*, 2 h, 4 h, 6 h, and 8 h, were selected for the nitriding process with a nitriding temperature of 800 °C. The samples were expressed as N-HZSM-5-2 h, N-HZSM-5-4 h, N -HZSM-5-6 h, and N-HZSM-5-8 h, respectively. With the extension of the nitriding time, the nitrogen content of the HZSM-5 sieve gradually increased, and the nitrogen content reached up to 0.76 wt% at 8 h. The specific surface area and pore volume both showed a downward trend. When the nitriding time was longer (8 h), the decrease was more obvious, and the specific surface area and pore volume decreased to 314 $m^2/g$ and 0.20 $cm^3/g$, respectively. The average pore diameter increased as the nitriding time increased and reached a maximum value (2.82 nm) at 8 h.

To further evaluate the effect of nitridation on the crystal structure of HZSM-5, XRD tests were performed on the N-HZSM-5 sieve obtained under different nitriding conditions. Figures 1a and 1b show that with the increase in nitriding temperature or the extension of the nitriding time, the intensity of some of the XRD peaks of the HZSM-5 molecular sieve underwent some changes. The intensity of the diffraction peak of $2\theta$ in the range of 22° to 25° slightly decreased, while the intensity of the diffraction peak of $2\theta$ in the range of 7.5° to 8.5° considerably increased, which indicated that the zeolite structure

slightly changed during the nitriding process. When the nitriding temperature was 900 °C, the diffraction peak intensity of the molecular sieve crystal clearly weakened after ammonia treatment, probably because a small amount of molecular sieve crystal lattice collapses during the nitriding process. A decrease in the specific surface area of the N-HZSM-5-900 sample (Table 1) also confirms this assumption. The SEM images (Fig. 2) also shows that the morphologies of the HZSM-5 and N-HZSM-5-6 h samples were slightly different. As such, it was shown that nitriding shortens the grain size.

Therefore, the analysis based on these results showed that the structure of the HZSM-5 sieve will change as the nitriding temperature or nitriding time is increased. This is likely because the $NH_3$ reacted with the hydroxyl groups on the surface of the HZSM-5 sieve during the nitridation process, which caused slight damage to the microporous structure.

**Table 1.** Effect of Nitriding on the Texture Properties of HZSM-5

| Catalyst | Nitrogen Content (wt%) | Pore Volume ($cm^3/g$) | Surface Area ($m^2/g$) | Average Pore Diameter (nm) |
|---|---|---|---|---|
| HZSM-5 | 0 | 0.24 | 356.10 | 2.61 |
| N-HZSM-5-600 | 0.25 | 0.23 | 348.02 | 2.68 |
| N-HZSM-5-700 | 0.41 | 0.23 | 344.22 | 2.70 |
| N-HZSM-5-800 | 0.66 | 0.22 | 342.59 | 2.72 |
| N-HZSM-5-900 | 0.54 | 0.21 | 325.32 | 2.75 |
| N-HZSM-5-2 h | 0.56 | 0.23 | 346.10 | 2.64 |
| N-HZSM-5-4 h | 0.66 | 0.22 | 342.59 | 2.72 |
| N-HZSM-5-6 h | 0.73 | 0.22 | 325.75 | 2.80 |
| N-HZSM-5-8 h | 0.76 | 0.20 | 313.53 | 2.82 |

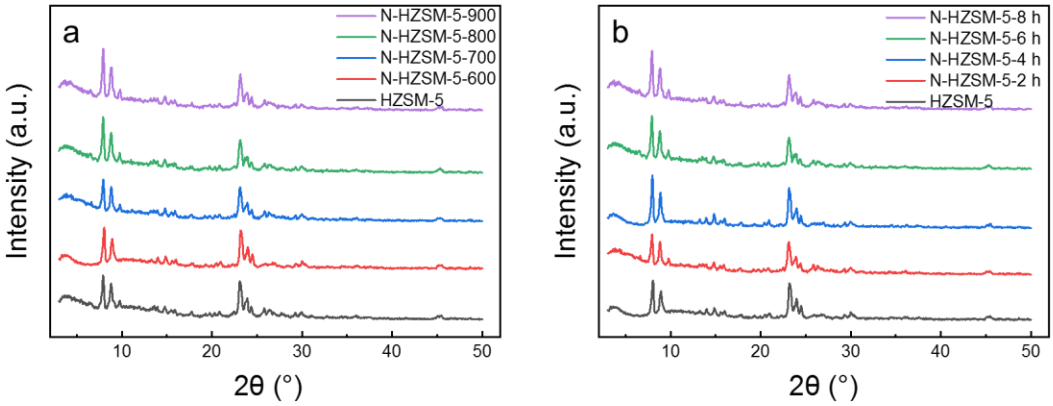


**Fig. 1.** XRD of the HZSM-5 and N-HZSM-5 sieves: a) at different nitriding temperatures; and b) at different nitriding times

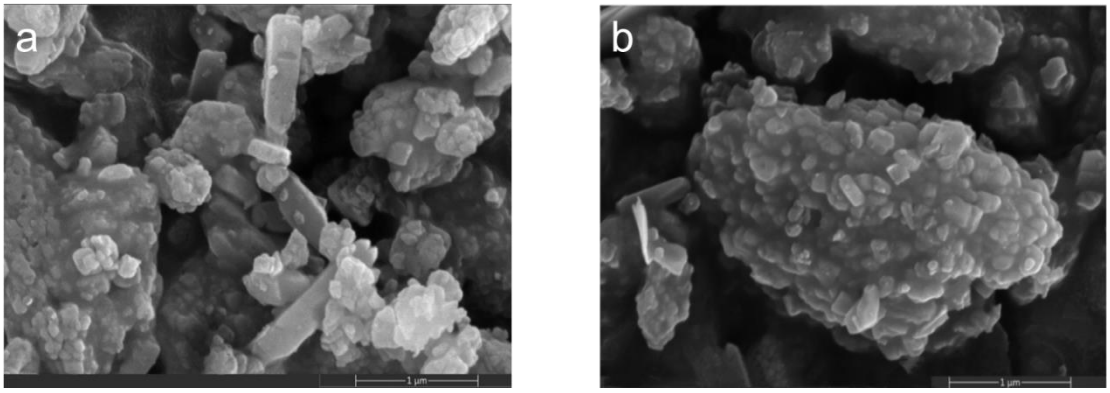


**Fig. 2.** SEM images of a) HZSM-5; and b) N-HZSM-5-6 h

## Effect of Nitriding on the Acidity of HZSM-5

According to Figs. 3a and 3b, the HZSM-5 molecular sieve before nitriding showed two obvious $NH_3$ desorption peaks, and their corresponding desorption temperatures were approximately 180 and 400 °C, which correspond to the desorption of $NH_3$ at the weak acidic and strong acidic sites on the surface of the HZSM-5 molecular sieve, respectively. Notably, on the $NH_3$-TPD curve of the molecular sieve after nitriding, the $NH_3$ desorption peak at the strong acidic site on the surface of the molecular sieve considerably changed. As the nitriding temperature or nitriding time increased, the change in the molecular sieve became more and more obvious. Not only did the number of acid sites decrease, but the acid strength also decreased, and the original $NH_3$ desorption peak almost completely disappeared. However, the peak area corresponding to the desorption peak of $NH_3$ at the weak acidic site on the surface of the molecular sieve tended to increase and then decrease, but the change was minimal. Although the $NH_3$ temperature-programmed desorption characterization can be used to obtain the strength and number of acid sites on the zeolite surface before and after nitridation, the type and number of acid sites on the zeolite surface cannot be obtained. Therefore, a pyridine adsorption infrared spectroscopy (Py-IR) test was conducted on the HZSM-5 sieve before and after nitriding. Table 2 shows that after the HZSM-5 sieve was nitrided, the amount of Brønsted acid sites (BASs) was greatly reduced, and as the nitriding temperature or nitriding time increased, the decrease in BASs became greater. When studying the nitriding temperature, the BASs content was the lowest at a nitriding temperature of 900 °C (36.07 μmol/g). When studying the nitriding time, the BASs content was the lowest at a nitriding time of 8 h (43.33 μmol/g). However, the nitriding process increases the Lewis acid sites (LASs) content; the LASs showed a trend of first increasing and then decreasing. When the nitriding temperature reached 800 °C, the LASs content reached 180.47 μmol/g; the maximum LASs content was 189.47 μmol/g when the nitriding time was increased to 6 h. Guan *et al*. (2006) reported that after the HZSM-5 molecular sieve was nitridated, the strong acidity of the molecular sieve considerably changed, primarily because the nitrogen atoms partially replaced the oxygen atoms connected to the skeleton Si atoms during the nitridation process. This phenomenon reduced the surface hydroxyl groups of the molecular sieve, thereby changing the acidity of the molecular sieve.

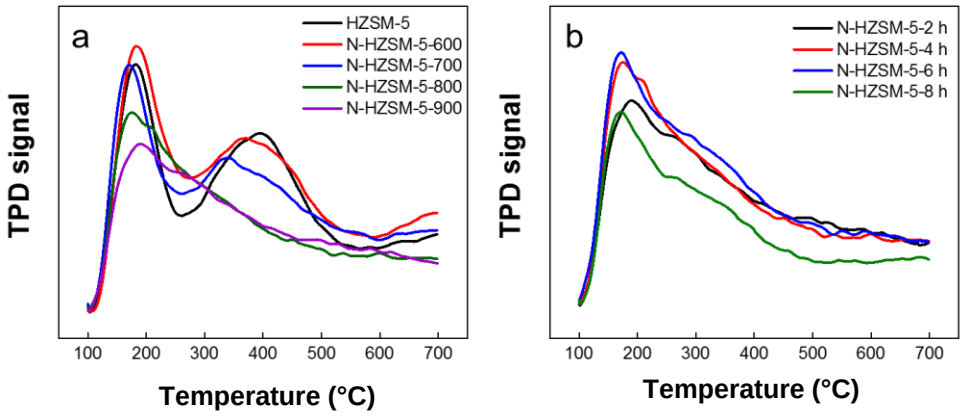


**Fig. 3.** $NH_3$-TPD diagrams of a) HZSM-5 and N-HZSM-5 at different nitriding temperatures; and b) N-HZSM-5 at different nitriding times

**Table 2.** Py-IR Results of the HZSM-5 and N-HZSM-5 Sieves

| Catalyst | Acid Amount (μmol/g) | | | Brønsted to Lewis Ratio |
|---|---|---|---|---|
| | Brønsted acid | Lewis acid | Total | |
| HZSM-5 | 323.41 | 106.66 | 430.07 | 3.03 |
| N-HZSM-5-600 | 152.14 | 157.20 | 309.33 | 0.97 |
| N-HZSM-5-700 | 93.98 | 159.44 | 253.42 | 0.60 |
| N-HZSM-5-800 | 69.57 | 180.47 | 250.04 | 0.38 |
| N-HZSM-5-900 | 36.07 | 153.40 | 189.47 | 0.24 |
| N-HZSM-5-2 h | 70.06 | 137.37 | 207.43 | 0.51 |
| N-HZSM-5-4 h | 69.57 | 180.47 | 250.04 | 0.39 |
| N-HZSM-5-6 h | 59.18 | 189.47 | 248.65 | 0.31 |
| N-HZSM-5-8 h | 43.33 | 164.91 | 208.23 | 0.26 |

## Effect of Different Nitriding Temperatures on the Selectivity of Furfural

Under the conditions of a CA to CL ratio of 2 and a pyrolysis temperature of 500 °C, the product distribution of cellulose pyrolysis with and without a catalyst was compared. Prior to this, extensive studies have been conducted on the pyrolysis of pure cellulose, and the results were consistent with the previous results by Rutkowski (2012). Levoglucan is the primary product with a selectivity of above 60%, and various other organic compounds including LAC, DGP, and furfural are also produced. As shown in Fig. 4a, the furfural selectivity of the noncatalytic process is 1.2%, and the LG selectivity is 66%. When HZSM-5 is used in the catalytic pyrolysis of cellulose, the product distribution considerably changed. Many aromatic hydrocarbon products were produced, primarily benzene, naphthalene, toluene, and dimethyl naphthalene, with a selectivity of up to 30.24%. At the same time, the LG selectivity was considerably reduced (26.87%). Although the selectivity of FF was increased to 3.6%, it is still not considered high enough. When N-HZSM-5 was added, its catalytic effect was considerably different from HZSM-5. As the nitriding temperature was increased, the aromatic selectivity decreased from 30.24% to 4.28%. The selectivity of LG first decreased from 26.87% to 20.17% and then increased to 23.43%. The selectivity of FF first increased from 3.6% to 12% and then decreased to 10%. At a nitriding temperature of 800 °C, the selectivity of FF was the

highest (12%). This is likely due to the fact that as the nitriding temperature increases, the BASs content gradually decreased, thus inhibiting the further cracking of furan compounds into aromatic hydrocarbons, thereby increasing the selectivity of FF and reducing the selectivity of aromatic hydrocarbons (Lee *et al.* 2013). At the same time, an increase in LASs will also promote the decomposition of LG to form FF (Lima *et al*. 2010). When the nitriding temperature was 800 °C, the LASs content was the highest, and the selectivity of furfural is also the highest. As the nitriding temperature continued to increase, *i.e.*, to 900 °C, not only did the LASs content decrease, but the specific surface area also decreased. Therefore, the selectivity of FF was reduced, because the distribution of active sites will also be affected by structural properties, *i.e.*, specific surface area, pore size, *etc.* (Zhang *et al*. 2020).

## Effect of Different Nitriding Times on the Selectivity of Furfural

Figure 4b shows the effect of the nitriding time on the product selectivity when the CA to CL ratio was 2 and the nitriding temperature was 800 °C. As the nitriding time increased, the aromatic selectivity decreased from 9.71% to 4.60%; the selectivity of LG first decreased from 25.70% to 18.65% and then increased to 22.54%, while the selectivity of FF first increased from 9% to 15% and then decreased to 13%. When the nitriding time was 6 h, the selectivity of FF was the highest (15%). When the nitriding time was increased to 8 h, the selectivity of FF decreased (13%). Since the LASs content was reduced, the amount of FF generated *via* LG cracking was reduced, which led to a decrease in the amount of FF and an increase in the amount of LG. However, as the nitriding time increased, the BASs content showed a downward trend, so the selectivity of the aromatic hydrocarbons continued to decrease. The existence of acid centers is a necessary condition for the production of FF; to achieve the maximum selectivity of FF, it is necessary to select the appropriate acid strength, number, and type of acid centers.

Based on the above analysis results, it was found that a nitriding temperature of 800 °C and a nitriding time of 6 h were the optimal nitriding conditions for the preparation of FF, and the selectivity of FF reached up to 15%.

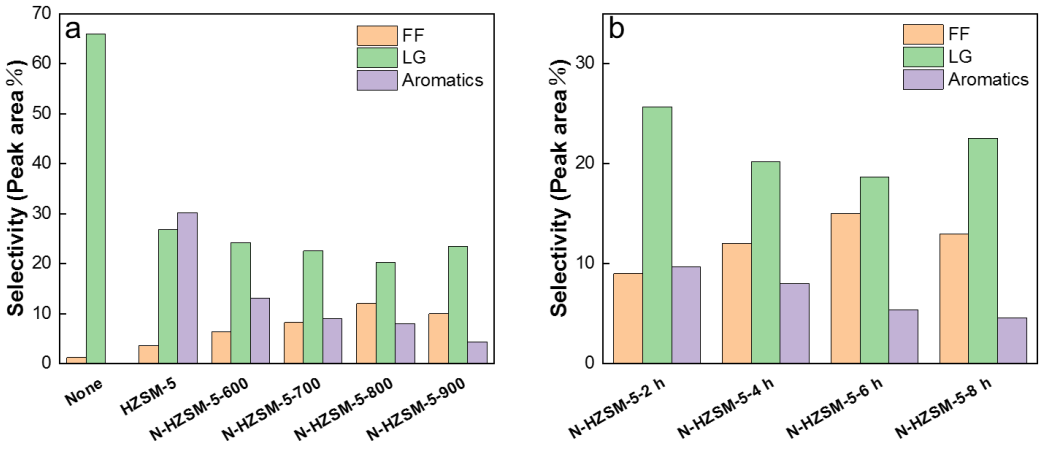


**Fig. 4.** The selectivity of different catalysts for FF, LG, and various aromatics in: a) pure cellulose, HZSM-5, and N-HZSM-5 at different nitriding temperatures; and b) N-HZSM-5 at different nitriding times

## Effect of the CA to CL Ratio on Furfural Selectivity

The CA to CL ratio is also an important factor affecting the product selectivity. Figure 5 shows the effect of a nitriding temperature of 800 °C and a nitriding time of 6 in conjunction with different CA to CL ratios on the selectivity of aromatic hydrocarbons, LG, and FF. As the CA to CL ratio increased, the selectivity of aromatic hydrocarbons increased from 4.6% to 10%. The selectivity of LG first decreased from 34% to 6.6% and then it increased to 15%. However, the selectivity of FF first increased from 12.8% to 24% and then it decreased to 20%. When the CA to CL ratio was 4, the selectivity of FF was the highest (24%). As the CA to CL ratio continued to increase, the selectivity of FF decreased to 20%. This was likely due to the fact that when the CA to CL ratio was less than 4, the N-HZSM-5 content was less, which cannot provide enough active sites, thus limiting the catalysis of FF formation. When the CA to CL ratio was greater than 4, the selectivity of FF decreased, which was likely caused by the limited heat and mass transfer in the reaction process caused by additional catalysts. However, as the CA to CL ratio increased, the selectivity of aromatic hydrocarbons also increased, which may be due to the increase in the N-HZSM-5 content, which provides additional B acidic sites and more uniform contact, which leads to an increase in selectivity. In addition, with the increase in the CA to CL ratio, the bio-oil yield increased from 28% to 71%, the gas yield decreased from 62% to 20%, and the coke yield decreased from 14% to 10%. The lower coke yield can alleviate the surface carbon behavior of N-HZSM-5 to a certain extent, which is beneficial to improve the service life of molecular sieve catalysts.

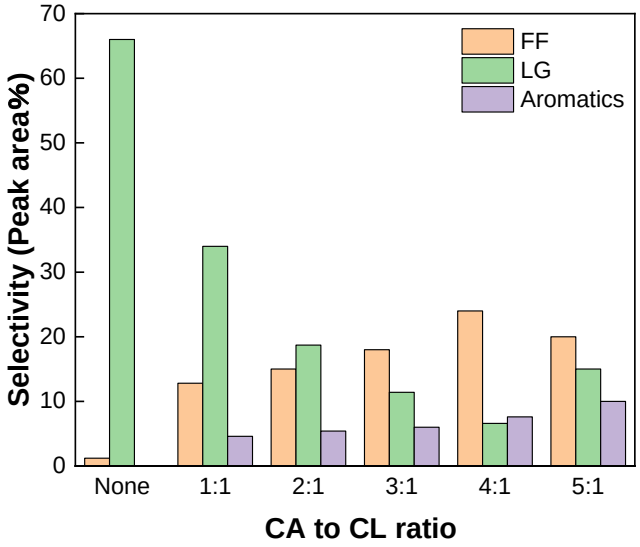


**Fig. 5.** Effect of the CA to CL ratio on the selectivity of FF, LG, and Aromatics

## Reaction Pathway from Cellulose to Furfural Under N-HZSM-5 Catalysis

During the pyrolysis process, cellulose decomposes primarily *via* competing depolymerization, dehydration, and fragmentation reactions, and the primary decomposition product is LG (Rutkowski 2012; Zhang *et al*. 2017). The LG peak area % during the noncatalytic cellulose pyrolysis process was 66%, but under the catalysis of N-HZSM-5, LG almost disappeared, which was consistent with the effect of an acidic catalyst on LG (Adam *et al*. 2005). Many other studies have also shown that a proper Lewis acid

catalyst can increase the yield of FF and reduce the yield of LG (Lima *et al*. 2010; Bhaumik and Dhepe 2013). Therefore, N-HZSM-5 promotes the secondary cracking of LG to produce FF, which is a part of the reason for the increased selectivity of FF. In addition, Jeon *et al*. (2013) found that the presence of acid centers during the catalytic pyrolysis process is critical to the production of FF. Torri and Fabbri (2009) believed that when the acidic sites are strong BASs, the FF generated *via* LG cracking can be converted into aromatic compounds for the second time. Therefore, the high LASs content of N-HZSM-5 promoted the cleavage of LG to FF, and the low BASs content inhibited the secondary conversion of FF to aromatic compounds. Therefore, the N-HZSM-5-catalyzed pyrolysis of cellulose considerably improved the selectivity of FF.

## CONCLUSIONS

1. In this study, a new type of N-HZSM-5 solid acid catalyst was prepared for the highly selective preparation of furfural from the catalytic pyrolysis of cellulose. The N-HZSM-5-6 h had a higher specific surface area (326 $m^2$/g), a larger average pore size (2.80 nm), more Lewis acid sites (LASs) (189.47 μmol/g) and lower Brønsted acid sites (BASs) (59.18 μmol/g), which considerably improved the catalytic activity of cellulose.
2. With the increase in nitriding temperature, nitriding time, and catalyst (CA) to cellulose (CL) ratio, the selectivity for furfural (FF) first increased and then decreased. The optimal conditions for the synthesis of furfural are as follows: a nitriding temperature of 800 °C, a nitriding time of 6 h, and a CA to CL ratio of 4. The maximum selectivity of FF was 24%, compared with HZSM-5 catalyzed pyrolysis of cellulose, the selectivity of FF is increased by 8 times.
3. Compared with HZSM-5, N-HZSM-5 presented higher catalytic activity for FF during pyrolysis. The N-HZSM-5 with appropriate acidity synergistically promoted the cleavage of LG to produce FF and inhibited the secondary conversion of FF to aromatic hydrocarbon compounds. Therefore, N-HZSM-5 has broad application prospects in the preparation of FF *via* cellulose pyrolysis with high selectivity.

## ACKNOWLEDGEMENTS

This research was sponsored by the National Key Research and Development Program of China (No. 2019YFD1100600), the National Natural Science Foundation of China (No. 51536009 and No. 51606113), the Shandong Provincial Natural Science Foundation, China (No. ZR2020ME184) and the distinguished expertise of the Taishan scholars of the Shandong Province.

## REFERENCES CITED

Adam, J., Blazsó, M., Mészáros, E., Stöcker, M., Nilsen, M. H., Bouzga, A., Hustad, J. E., Grønli, M., and Øye, G. (2005). "Pyrolysis of biomass in the presence of Al-MCM-41 type catalysts," *Fuel* 84(12-13), 1494-1502. DOI: 10.1016/j.fuel.2005.02.006

Bhaumik, P., and Dhepe, P. L. (2013). "Efficient, stable, and reusable silicoaluminophosphate for the one-pot production of furfural from hemicellulose," *ACS Catalysis* 3(10), 2299-2303. DOI: 10.1021/cs400495j

Blasco, T., Corma, A., Fernández, L., Forne′s, V., and Guil-López, R. (1999). "Magic angle spinning NMR investigations on amorphous aluminophosphate oxynitrides," *Physical Chemistry Chemical Physics* 1(18), 4493-4499. DOI: 10.1039/A904244J

Cai, C. M., Zhang, T., Kumar, R., and Wyman, C. E. (2013). "Integrated furfural production as a renewable fuel and chemical platform from lignocellulosic biomass," *Journal of Chemical Technology and Biotechnology* 89(1), 2-10. DOI: 10.1002/jctb.4168

Chen, X., Chen, Y., Chen, Z., Zhu, D., Yang, H., Liu, P., Li, T., and Chen, H. (2018). "Catalytic fast pyrolysis of cellulose to produce furan compounds with SAPO type catalysts," *Journal of Analytical and Applied Pyrolysis* 129, 53-60. DOI: 10.1016/j.jaap.2017.12.004

Chen, X., Yang, H., Chen, Y., Chen, W., Lei, T., Zhang, W., and Chen, H. (2017). "Catalytic fast pyrolysis of biomass to produce furfural using heterogeneous catalysts," *Journal of Analytical and Applied Pyrolysis* 127, 292-298. DOI: 10.1016/j.jaap.2017.07.022

Fabbri, D., Torri, C., and Mancini, I. (2007). "Pyrolysis of cellulose catalysed by nanopowder metal oxides: Production and characterisation of a chiral hydroxylactone and its role as building block," *Green Chemistry* 9(12), 1374-1379. DOI: 10.1039/b707943e

Fan, Y., Zhang, D., Zheng, A., Zhao, Z., Li, H., and Yang, T. (2018). "Selective production of anhydrosugars and furfural from fast pyrolysis of corncobs using sulfuric acid as an inhibitor and catalyst," *Chemical Engineering Journal* 358, 743-751. DOI: 10.1016/j.cej.2018.10.014

Fanchiang, W.-L., and Lin, Y.-C. (2012). "Catalytic fast pyrolysis of furfural over H-ZSM-5 and ZN/H-ZSM-5 catalysts," *Applied Catalysis A: General* 419-420, 102-110. DOI: 10.1016/j.apcata.2012.01.017

Gao, Z., Li, N., Chen, M., and Yi, W. (2019). "Comparative study on the pyrolysis of cellulose and its model compounds," *Fuel Processing Technology* 193, 131-140. DOI: 10.1016/j.fuproc.2019.04.038

Guan, X.-X., Li, N., Wu, G.-J., and Chen, J.-X. (2006). "Para-selectivity of modified HZSM-5 zeolites by nitridation for ethylation of ethylbenzene with ethanol," *Journal of Molecular Catalysis A Chemical* 248(1-2), 220-225. DOI: 10.1016/j.molcata.2005.12.032

Jeon, M.-J., Jeon, J.-K., Suh, D. J., Park, S. H., Sa, Y. J., Joo, S. H., and Park Y.-K. (2013). "Catalytic pyrolysis of biomass components over mesoporous catalysts using Py-GC/MS." *Catalysis Today* 204, 170-178. DOI: 10.1016/j.cattod.2012.07.039

Kabir, G., and Hameed, B. H. (2017). "Recent progress on catalytic pyrolysis of lignocellulosic biomass to high-grade bio-oil and bio-chemicals," *Renewable and Sustainable Energy Reviews* 70, 945-967. DOI: 10.1016/j.rser.2016.12.001

Lange, J.-P., Heide, E. v. d., Buijtenen, J. v., and Price, R. (2012). "Furfural-A promising platform for lignocellulosic biofuels," *ChemSusChem* 5(1), 66-150. DOI: 10.1002/cssc.201100648

Lee, H. W., Kim, T. H., Park, S. H., Jeon, J.-K., Suh, D. J., and Park, Y.-K. (2013). "Catalytic fast pyrolysis of lignin over mesoporous y zeolite using Py-GC/MS." *Journal of Nanoscience & Nanotechnology* 13(4), 2640-2646. DOI:

10.1166/jnn.2013.7421

Li, S., Li, S., Wang, C., and Zhu, X. (2020). "Catalytic effects of ammonium dihydrogen phosphate on the pyrolysis of lignocellulosic biomass: Selective production of furfural and levoglucosenone," *Fuel Processing Technology* 209, 1-11. DOI: 10.1016/j.fuproc.2020.106525

Li, Y., Li, K., Hu, B., Zhang, Z., Zhang, G., Feng, S., Wang, T., and Lu, Q. (2021). "Catalytic fast pyrolysis of cellulose for selective production of 1-hydroxy-3,6-dioxabicyclo[3.2.1]octan-2-one using nickel-tin layered double oxides," *Industrial Crops and Products* 162, 113-269. DOI: 10.106/j.indcrop.2021.113269

Liang, T., Wang, S. R., Guo, X. J., Zhou, Y., and Gu, Y. L. (2011). "Catalytic fast pyrolysis of cellulose with HZSM-5," *Advanced Materials Research* 347-353, 2459-2463. DOI: 10.4028/www.scientific.net/AMR.347-353.2459

Lima, S., Fernandes, A., Antunes, M. M., Pillinger, M., Ribeiro, F., and Valente, A. A. (2010). "Dehydration of xylose into furfural in the presence of crystalline microporous silicoaluminophosphates," *Catalysis Letters* 135(1-2), 41-47. DOI: 10.1007/s10562-010-0259-6

Lu, Q., Dong, C., Zhang, X., Tian, H., Yang, Y., and Zhu, X. (2011a). "Selective fast pyrolysis of biomass impregnated with $ZnCl_2$ to produce furfural: Analytical Py-GC/MS study," *Journal of Analytical & Applied Pyrolysis* 90(2), 204-212. DOI: 10.1016/j.jaap.2010.12.007

Lu, Q., Liao, H., Zhang, Y., Zhang, J., and Dong, C. (2013). "Reaction mechanism of low-temperature fast pyrolysis of fructose to produce 5-hydroxymethyl furfural," *Journal of Fuel Chemistry and Technology* 41(9), 1070-1076. DOI: 10.1016/S1872-5813(13)60044-4

Lu, Q., Yang, X., Dong, C., Zhang, Z., Zhang, X., and Zhu, X. (2011b). "Influence of pyrolysis temperature and time on the cellulose fast pyrolysis products: Analytical Py-GC/MS study," *Journal of Analytical and Applied Pyrolysis* 92(2), 430-438. DOI: 10.1016/j.jaap.2011.08.006

Lyu, J.-H., Hu, H. -L., Rui, J. -Y., Zhang, Q. -F., Cen, J., Han, W. -W., Wang, Q. -T., Chen, X. -K., Pan, Z. -Y., and Li, X. -N. (2017). "Nitridation: A simple way to improve the catalytic performance of hierarchical porous ZSM-5 in benzene alkylation with methanol," *Chinese Chemical Letters* 28(2), 482-486. DOI: 10.1016/j.cclet.2016.10.025

Narasimharao, K., Hartmann, M., Thiel, H. H., and Ernst, S. (2006). "Novel solid basic catalysts by nitridation of zeolite beta at low temperature," *Microporous and Mesoporous Materials* 90(1-3), 377-383. DOI: 10.1016/j.micromeso.2005.11.029

Razzaq, M., Zeeshan, M., Qaisar, S., Iftikhar, H., and Muneer, B. (2019). "Investigating use of metal-modified HZSM-5 catalyst to upgrade liquid yield in co-pyrolysis of wheat straw and polystyrene," *Fuel* 257, 116-119. DOI: 10.1016/j.fuel.2019.116119

Rutkowski, P. (2012). "Pyrolytic behavior of cellulose in presence of montmorillonite K10 as catalyst," *Journal of Analytical and Applied Pyrolysis* 98, 115-122. DOI: 10.1016/j.jaap.2012.07.012

Shahsavari, S., and Sadrameli, S. M. (2020). "Production of renewable aromatics and heterocycles by catalytic pyrolysis of biomass resources using rhenium and tin promoted ZSM-5 zeolite catalysts," *Process Safety and Environmental Protection.* 141, 305-320. DOI: 10.1016/j.psep.2020.04.023

Torri, C., and Fabbri, D. (2009). "Analytical study on the pyrolytic behaviour of cellulose in the presence of mcm-41 mesoporous materials," *Journal of Analytical and Applied*

*Pyrolysis* 85(1-2), 192-196. DOI: 10.1016/j.jaap.2008.11.024

Veses, A., Puértolas, B., Callén, M. S., and García, T. (2015). "Catalytic upgrading of biomass derived pyrolysis vapors over metal-loaded ZSM-5 zeolites: Effect of different metal cations on the bio-oil final properties," *Microporous and Mesoporous Materials* 209, 189-196. DOI: 10.1016/j.micromeso.2015.01.012

Zhang, H., Liu, X., Lu, M., Hu, X., Lu, L., Tian, X., and Ji, J. (2014). "Role of Brønsted acid in selective production of furfural in biomass pyrolysis," *Bioresource Technology* 169, 800-803. DOI: 10.1016/j.biortech.2014.07.053

Zhang, H., Meng, X., Liu, C., Wang, Y., and Xiao, R. (2017). "Selective low-temperature pyrolysis of microcrystalline cellulose to produce levoglucosan and levoglucosenone in a fixed bed reactor," *Fuel Processing Technology* 167, 484-490. DOI: 10.1016/j.fuproc.2017.08.007

Zhang, S., Zhang, H., Liu, X., Zhu, S., Hu, L., and Zhang, Q. (2018). "Upgrading of bio-oil from catalytic pyrolysis of pretreated rice husk over Fe-modified ZSM-5 zeolite catalyst," *Fuel Processing Technology* 175, 17-25. DOI: 10.1016/j.fuproc.2018.03.002

Zhang, Z., Hu, B., Li, Y., Li, K., and Lu, Q. (2020). "Selective preparation of 1-hydroxy-3,6-dioxabicyclo[3.2.1]octan-2-one by fast pyrolysis of cellulose catalyzed with metal-loaded nitrided HZSM-5," *Bioresource Technology* 309, 1-8. DOI: 10.1016/j.biortech.2020.123370

Article submitted: July 4, 2021; Peer review completed: August 28, 2021; Revised version received: September 1, 2021; Accepted: September 22, 2021; Published: September 27, 2021.
DOI: 10.15376/biores.16.4.7578-7591